Steel Structures Research Update

Slotted-Hidden-Gap Connections and Intentional Eccentricity for Steel Brace Members

JUDY LIU

INTRODUCTION

Research on alternatives for steel brace members and their connections is highlighted. These studies are a collaboration between Dr. Colin Rogers, Professor and Acting Chair at McGill University, and Dr. Robert Tremblay, Professor at Polytechnique Montreal. Dr. Rogers's research interests include structural steel connections, seismic design of low-rise steel buildings, lateral-force-resisting systems for cold-formed steel structures, and seismic-deficient braced steel frames. Dr. Tremblay's research interests include seismic design, dynamic analysis and stability of structures, steel, and steel-concrete structures. Dr. Tremblay was recognized in 2022 with AISC's Lifetime Achievement Award for significant contributions to the development of steel design standards and the advancement of seismic design of steel structures, including braced frames. Service contributions for Dr. Rogers and Dr. Tremblay include their work on the Canadian Standards Association (CSA) S16 Design of Steel Structures committee. Some of the research team's investigations into novel approaches for steel brace and connection design are presented, along with a preview of future work.

BRACES WITH INTENTIONAL ECCENTRICITY

Research on braces with intentional eccentricity (BIEs) is motivated by improvements in seismic performance compared to concentrically loaded brace (CLB) members. A brief summary of the background, motivation, and research objectives is presented. Also provided are selected highlights of the experimental program and supplementary finite element study.

Disadvantages for concentrically braced frames (CBFs) stem from stiffness and overstrength. The frames see high spectral acceleration demands and therefore large design forces due to their initial lateral stiffness. The concentrically loaded brace (CLB) members are sized based on their compression resistance. The resulting overstrength creates challenges in capacity design, as other CBF members and components are designed to resist the expected, or probable, strength of the CLBs. Additional overstrength is due to seismic width-to-thickness limits, established to improve frame ductility and energy dissipation by delaying local buckling and eventual fracture at mid-length plastic hinge region. Meanwhile, CBFs experience low lateral stiffness as the braces yield in tension and buckle in compression. This behavior can concentrate in one story or a limited number of stories, leading to large lateral drifts and the potential for a soft-story mechanism.

The introduction of eccentricity in the brace can improve the seismic behavior. Skalomenos et al. (2017) are credited with the initial concept of offsetting the brace longitudinal axis from the line of force, as shown in Figure 1. The eccentricity produces bending in addition to axial force and results in a lower initial stiffness. Rather than yielding uniformly over the cross section, yielding begins at the extreme fiber. The subsequent progression of yielding through the cross section results in a greater post-yield stiffness. The flexural response also "induces a more even distribution of the strain demands over the brace length, instead of an earlier strain concentration at mid-length as in CLBs" (González Ureña et al., 2022). So, the onset of local buckling is delayed, increasing the fracture life of the brace. The eccentricity can be tuned to the desired initial and post-yield stiffness. The eccentricity can also be adjusted at specific stories to achieve a design with a "smoother distribution of drift demands over the building height" (González Ureña et al., 2022). For a detailed analysis of the force-deformation response of a BIE, refer to González Ureña et al. (2022).

The potential benefits of braces with intentional eccentricity are supported by system analyses conducted by the research team. González Ureña et al. (2021) investigated the seismic design and performance of frames with intentionally eccentric braces (FIEBs). The study included nonlinear time-history analyses of 4-, 8-, and 12-story prototype buildings designed with FIEBs for high-seismic demands. Maximum and residual story drifts were "significantly lower, owing to the substantial secondary stiffness of BIEs" (González Ureña et al., 2021). Also, the study demonstrated that BIEs can be used to avoid the concentrically braced frame tendency to concentrate drift demands within a story

Judy Liu, PhD, Research Editor of the AISC *Engineering Journal*, Professor, Oregon State University, School of Civil and Construction Engineering, Corvallis, Ore. Email: judy.liu@oregonstate.edu

or limited number of stories. Refer to González Ureña et al. (2021) for additional conclusions and commentary on the FIEB design.

The most recent work by the research team fills an important gap in knowledge for BIEs. Skalomenos et al. (2017) tested five half-scale BIE specimens using circular HSS and two different eccentricity values. Though the potential of BIEs has been demonstrated, there have been "no published reports on physical performance of full-scale nor square HSS BIE specimens" (González Ureña et al., 2022). The team therefore tested full-scale square ASTM A1085/A1085M (ASTM, 2015) HSS BIE and CLB specimens under cyclic loading. One specific research objective was to evaluate the "response of BIEs complying with and exceeding the CSA S16-14 limits for global and local slenderness" (González Ureña et al., 2022). Supplementary finite element (FE) models of CLBs and BIE extended the work, providing a look ahead to design of frames with intentionally eccentric braces (FIEBs). Refer to González Ureña et al. (2022) for a detailed presentation and discussion of the FE models and results.

Highlights of the Experimental Program

Test specimen details were based on current specifications and a prototypical frame. The team referenced CSA S16-14 (CSA, 2019) global and local slenderness limits for rectangular HSS CLBs. Dimensions were based on a 19.7 ft × 13.1 ft frame. Specimen 1 was a 5-in.-square, 0.315-in.-thick (HSS 127×127×8) CLB, for comparison with the BIE specimens. Specimen 2 was a BIE the same HSS section as Specimen 1 but with an eccentricity of 5.12 in. Specimens 3 and 5 were 10-in.-square, 0.512-in.-thick (HSS 254×254×13) BIEs, tested to determine if eccentricity could improve brace behavior. For these two specimens, the global slenderness was below the CSA S16-14 lower limit of 70. González Ureña et al. (2022) noted that the lower limit is "intended to preclude overly stocky braces, as low global slenderness is correlated with a higher probability of undesirable premature fracture." The width-to-thickness ratios (local slenderness) satisfied CSA limits. Specimens 3 and 5 had eccentricities of 7.87 in. and 11.8 in, respectively. Specimen 4 was a thinner-wall version of Specimen 3. For this 10-in.-square, 0.394-in.-thick (HSS 254×254×10) BIE, the local slenderness was greater than allowed by CSA S16-14.

The test setup was designed to represent a prototypical FIEB. To create the eccentricity, an "eccentering" assembly of two side plates welded to corners of the HSS connected the brace to a knife plate, as shown in Figure 2. The knife plate was detailed to act like a pinned connection, allowing out-of-plane rotation with buckling of the brace. The knife plate was then slotted onto a gusset plate and connected with four bolted angles. The cyclic loading history applied increasing displacements based on equivalent interstory drift of the prototypical 19.7 ft × 13.1 ft frame. For example, 1% drift corresponded to a brace axial displacement of 1.31 in. Refer to González Ureña et al. (2022) for more details of the test specimens, instrumentation, test set-up, and loading.

The behavior of Specimen 1 was as expected for a CLB. There was a "clear transition between the elastic and post-yielding stages in tension, a nearly constant post-yielding maximum force, and a distinct peak force in compression before its strength deteriorated due to global buckling" (González Ureña et al., 2022). The post-yield stiffness in tension was only about 1% of initial stiffness. Local buckling near mid-length began during the first 3% drift cycle in compression. Fracture due to low-cycle fatigue occurred during the second 4% drift cycle.

Specimen 2, the BIE version of Specimen 1, exhibited markedly different behavior in tension and compression. Specimen 2 had "significant post-yielding stiffness in

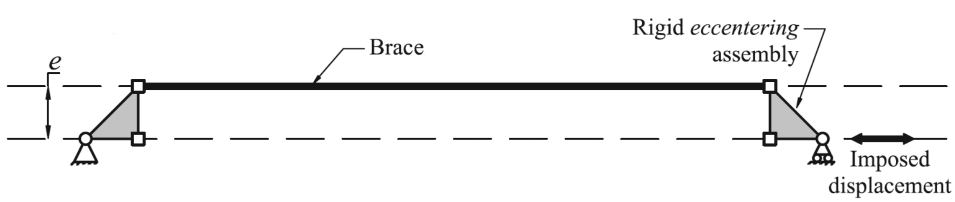

(a)

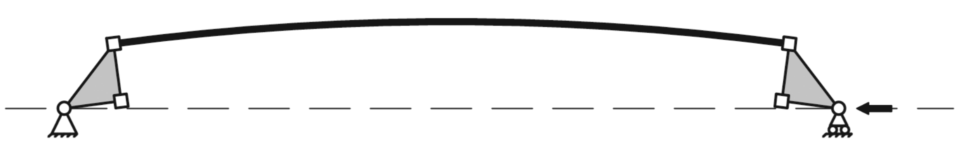

(b)

Fig. 1. (a) Components of a BIE and (b) deformed shape under compression.

tension, approximately 26% of the initial stiffness, and a smooth flexural response in compression, displaying neither global nor local buckling" (González Ureña et al., 2022). Specimen 2 achieved 58% of the theoretical tension yield capacity for the concentrically loaded Specimen 1. A decrease in the compression force after the peak was attributed to an increase in effective eccentricity due to bending. Specimen 2 started to fracture near the top eccentering assembly during first excursion to 2% drift in tension, with complete separation occurring during first 2.5% cycle. This failure mode would be studied further with the supplementary FE models.

Specimens 3, 4, and 5 all exhibited similar behavior, with local buckling and low-cycle fatigue fracture at brace mid-length. Specimen 5, with the same section but larger eccentricity than Specimen 3, had better fracture life (i.e., larger displacement) but lower initial stiffness and forces. Specimen 4 had the shortest fracture life of the three, due to its larger local slenderness. Initial stiffness and peak force values correlated to the cross-sectional areas for the three specimens, but post-yield stiffness was somewhat independent of the HSS properties.

The complementary FE models provided supplementary data as well as insight into the failure mode of Specimen 2. The fracture near the eccentering assembly revealed a shortcoming in the BIE configuration. A BIE under tension also experiences its largest flexural demands adjacent to the eccentering assemblies. From the FE model, Specimen 2, at time of failure, had reached its plastic bending moment capacity and about 71% of its maximum tensile strength. In another BIE FE model with the same failure mode, the BIE reached its plastic bending moment capacity and approximately 51% of its maximum tensile strength. In the BIE configuration used, the combined axial and flexural demands were being transmitted by welds along the corners of the HSS, where cold working and the heat of welding have affected the material ductility. González Ureña et al. (2022) considered that a configuration engaging the entire perimeter of the HSS would improve performance, but they also noted that Skalomenos et al. (2017) saw brittle failure with such a connection.

Given these results, the research team conducted an analysis of rotational demands at the ends of the HSS braces with the objective of developing design guidance. Noting limited data from this study and a lack of published work on rotational capacities of HSS under tension loading, they recommended that a conservative allowable rotation limit be used for HSS BIE design. The team suggested a provisional rotational limit of 10°. Refer to González Ureña et al. (2022) for more details of this analysis and recommendation.

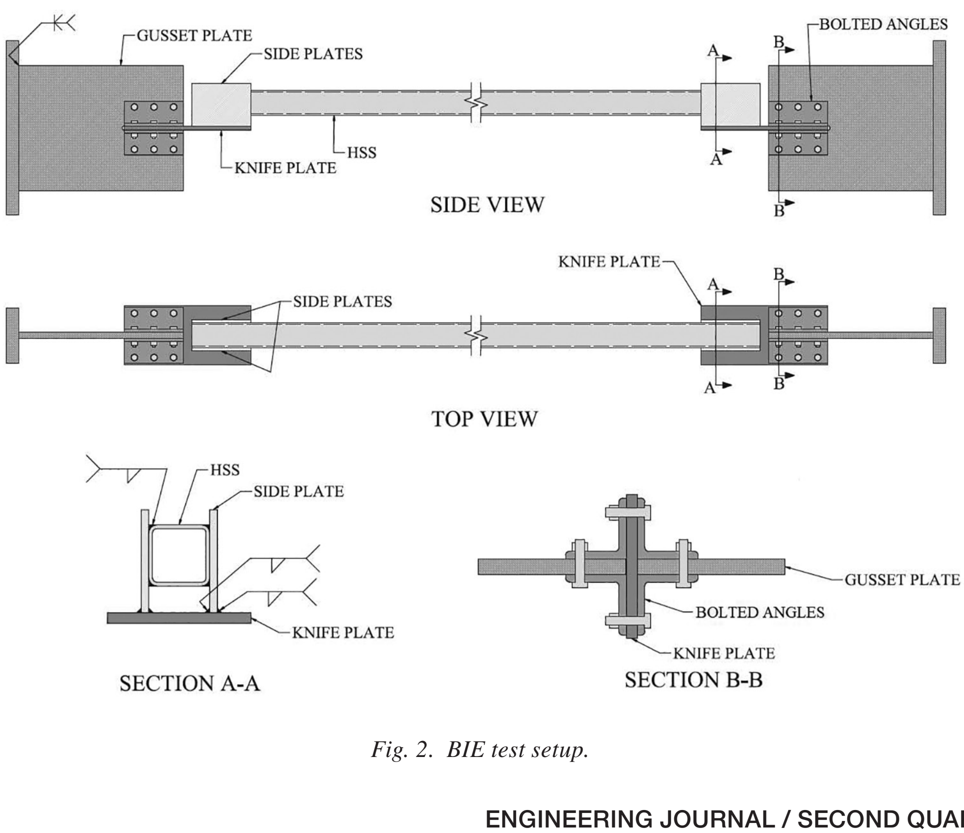

Fig. 2. BIE test setup.

Discussion

The highlighted work demonstrated the viability of BIEs and research needs. The BIE specimens "exhibited overall behavior and beneficial effects of the applied eccentricity, specifically substantial post-yielding stiffness and delayed onset of buckling at the brace mid-length" (González Ureña et al., 2022). The eccentricity can improve the fracture life of HSS braces that do not satisfy CSA S16-14 limits on global and local slenderness. Three BIE specimens had low-cycle fatigue-induced fracture at brace mid-length. One BIE fractured at the end, near the eccentering assembly, due to large rotation demands. More research is needed on allowable cyclic displacement capacities, especially at the ends of the BIEs. The research team recommends additional work focused on development of eccentering assemblies with lower rotational and strain demands on the HSS braces.

SLOTTED-HIDDEN-GAP CONNECTIONS

The slotted-hidden-gap (SHG) connection may eliminate the need to reinforce HSS braces at knife-plate connections, but existing design guidance is limited. The SHG prevents net section rupture of the HSS at the connection, promoting yielding throughout the brace length before rupture at midspan. Studies have confirmed the viability of the SHG connection, but the existing, empirical design approach was somewhat limited by available test data. Through an extensive, integrated program of numerical parametric studies and physical tests, the research team developed SHG connection design and detailing guidelines.

Characteristics of Slotted-Hidden-Gap Connections

The SHG connection differs from the conventional knife-plate connection in that both the HSS brace and gusset plate have slots. For the conventional connection, the gusset plate is inserted into slots on two sides of the HSS brace member and attached with fillet welds [Figure 3(a)]. This configuration locates the reduced net section of the HSS at the welds. The HSS also experiences shear lag and nonuniform tensile stresses at its reduced section. For the SHG connection, based on Mitsui et al. (1985), a slot is also cut into the gusset plate as shown in Figure 3(b). Mitsui et al. first introduced this "extended plate configuration" that, when assembled, allows the gusset plate and welds to extend past the ends of the HSS slots to the gross cross section (Figure 4). Stress concentrations are therefore moved away from the reduced net section. There is also a gap between the end of the HSS slot and the end of gusset plate slot.

A primary benefit to using SHG connections is that reinforcement of the net section is no longer needed. The HSS braces are the energy-dissipating fuses in the system, and capacity design principles require that the connection be stronger than the probable, or expected, strength of the brace. With an effective net section reduced by the slots and shear lag effects, section reinforcement (e.g., the addition of side plates) is typically necessary to satisfy capacity design requirements. The SHG connection, meanwhile, concentrates the inelastic demands away from the reduced section. In cyclic testing of braces or concentrically braced frames (CBFs) with SHG connections, Martinez-Saucedo et al. (2008), Packer et al. (2010), and Okazaki et al. (2013) did not observe any damage in the gusset plates, welds, or HSS net section. The main findings included confirmation that an increased weld length would reduce shear lag effects (Martinez-Saucedo et al., 2008) and that an SHG connection promotes extensive yielding in the brace with no fracture at the connection (e.g., Packer et al., 2010). These studies confirmed the viability of the SHG connection.

Research Objectives

The research team sought to improve seismic design and detailing methods for SHG connections. Existing guidance was "rather empirical and limited by the range of connection geometries and materials that had previously been tested" (Afifi et al., 2023). The work highlighted here builds from the research team's studies (Moreau et al., 2014; Afifi et al., 2021) that already provided insight into some details and brace behavior. For example, Moreau et al. (2014) recommended a minimum overlap length of 5% of the weld length as sufficient to develop the tensile yield resistance of the HSS brace. The study also showed net section fracture of conventional connections compared to yielding on the gross area for the braces with SHG connections. The load-transfer mechanism and effects of different parameters were extensively studied (e.g., Afifi et al., 2021). The work demonstrated the importance of a weld overlap length in avoiding net section rupture, benefits of smaller weld sizes and longer weld lengths, and the ability of SHG braced frame building models to achieve large interstory drift ratios (Afifi et al., 2021).

The team continued to investigate critical parameters—for example, weld configurations—and their effects on the performance of SHG connections in seismic applications. This work was accomplished through numerical parametric studies coordinated with an experimental program. Design and detailing recommendations were major outcomes of the research.

Numerical Parametric Study

Critical parameters investigated included the HSS size and thickness, weld overlap length, weld size and length, and gusset plate width and thickness. The study was organized in four parts. In Part 1, four 6-in.- to 12-in.-square

HSS were studied. Thickness was initially constant across the HSS, and then different thicknesses were investigated. Part 2 focused on the gusset plate thickness, ranging from 0.748 in. to 1.25 in. Part 3 examined welds approximately 10 in. to 24 in. long and weld size varying from 1.25 in. to 0.748 in. Part 4 focused on the overlap length—that is, the length of the weld on the gross cross-sectional area of the HSS. The overlap length was varied for a constant total weld length.

In the finite element (FE) model, solid elements and typical detailing and common grades of steel were used. First-order reduced-integration, hexahedral, eight-noded solid elements with hourglass control were used for the HSS, welds, and gusset plate. The HSS slot width was typically 0.118 in. greater than the plate thickness. Slots had rounded ends as is common detailing practice. HSS tubes were grade CSA G40.20-21, 350 W Class C (CSA, 2018) with nominal F_y = 51 ksi and F_u = 65 ksi. Plates were ASTM A572/A572M Gr. 50 (ASTM, 2021) with nominal F_y = 50 ksi and

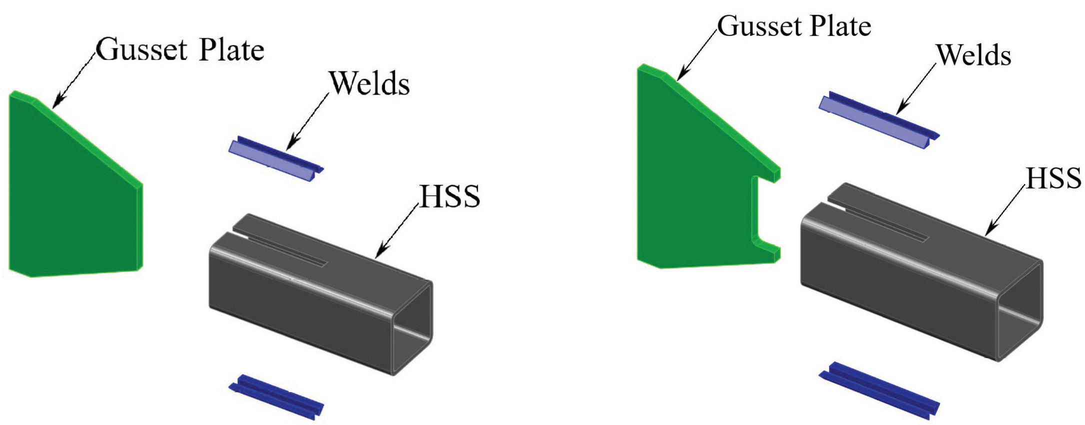

(a) Conventional *(b) Slotted-hidden-gap (SHG)*

Fig. 3. Exploded views of connection assemblies.

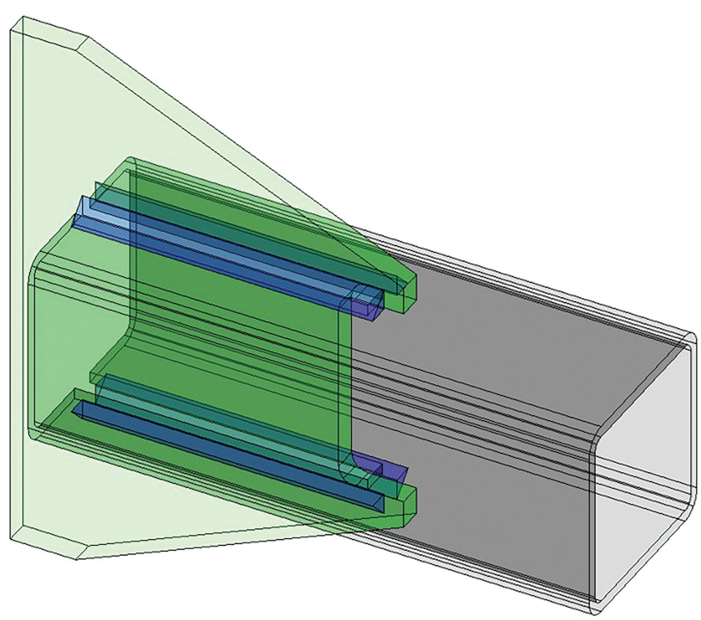

Fig. 4. X-ray view of slotted-hidden-gap (SHG) connection.

$F_u = 65$ ksi. For the welds, matching 71 ksi electrodes were used. For more FE model details, refer to Afifi et al. (2022).

The studies revealed how the different parameters affected the concentration of inelastic demands at the connections. The influence of HSS size and thickness is that larger sizes and thicknesses show more inelastic demands at the connection regions. As such, a larger weld overlap length may be needed to accommodate the increased connection stresses. Larger inelastic demands at the connection were also correlated to the thicker gusset plates. Meanwhile, smaller weld sizes and longer weld lengths resulted in a slight reduction in stresses at the connection. Finally, with a 0.787 in. weld overlap length, the desired SHG connection behavior was achieved. The study also revealed that the optimal weld overlap length is independent of the overall weld length. For more results and discussion, refer to Afifi et al. (2022).

Experimental Program

The experimental program and a companion FE study built upon the work by Moreau et al. (2014) and Afifi et al. (2021). Moreau et al. (2014) tested 4 conventional and 15 SHG connection specimens. Synthesis of the data and companion analyses by Afifi et al. (2021) revealed the influence of key parameters on the behavior of HSS braces with SHG connections as compared to conventional connections. The differences in the normalized load-deformation response and energy dissipation are clearly shown in Figure 5. The work also informed parameters requiring further investigation. The program described here expanded the range of applicability with brace and steel selection.

Test Specimens and Setup

This most recent work expanded the ranges for brace size and grade of steel. Specifically, 10-in.-square, 0.512-in.-thick (HSS 254×254×13) ASTM A1085/A1085M braces were used in this study. The HSS, the largest yet to be tested with the SHG connection, were chosen as they are typical of low- to medium-rise buildings in Canada (Afifi et al., 2022). With its relatively recent introduction to the market, A1085 steel is not commonly seen in published brace tests. Key parameters were tested with this extended range for HSS brace size and grade of steel.

The test program was designed to evaluate weld overlap length with consideration for the larger HSS and newer grade of steel. Specimens had SHG connections to paddle plates at both ends of HSS long enough to "allow for a uniform strain distribution at the central portion of the HSS brace" (Afifi et al., 2022) (Figure 6). Gusset plates were clamped by the grips of the loading device and were designed to remain elastic. Four bolted angles formed the gusset-paddle plate connection. For more details of the test set-up, refer to Afifi et al. (2022).

The two-part program investigated different weld configurations. The two specimens in Part 1 (weld configuration A) differed by the HSS slot length (15.2 in. vs. 15.9 in.) and the resulting weld overlap length (0.787 in. vs. 0 in.). Weld size and length were held constant at 1.14 in. and 15.4 in., respectively. In Part 2, longer, smaller welds (weld configuration B) were investigated. The weld size decreased from 1.14 in. to 0.748 in. Weld length increased from 15.4 in. to 24.4 in. The other parameters, such as weld overlap lengths, remained the same as in Part 1.

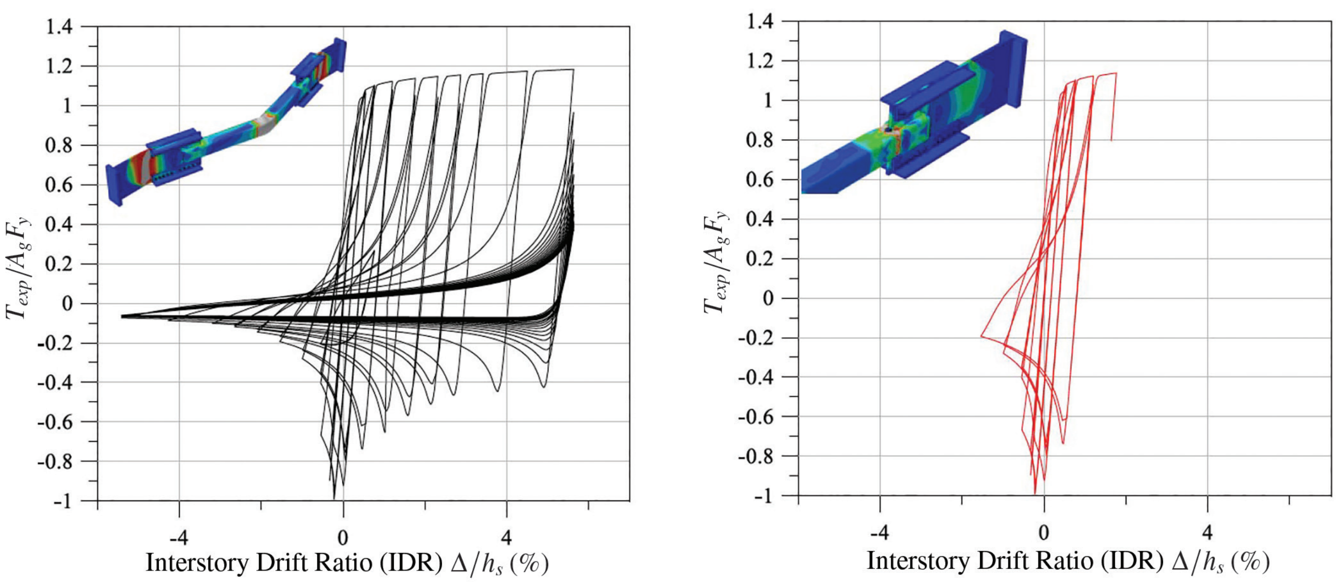

(a) SHG connection

(b) Conventional connection

Fig. 5. FE model comparisons of SHG and conventional connection normalized load-drift responses.

The specimens were loaded in tension and instrumented to capture the local strains as well as global force versus displacement. The specimens were monotonically and quasi-statically loaded so as to avoid strain rate effects. Instrumentation included the displacement transducer internal to the loading machine, string potentiometers for global and local displacements, strain gages, and a digital image correlation (DIC) system to capture local deformations. Additional details of the loading and instrumentation can be found in Afifi et al. (2022).

Results

The results from monotonic testing and companion FE models extended the range of applicability, supported prior conclusions, and provided additional insights into the behavior of HSS braces with SHG connections. As intended for these tests, inelastic behavior was limited to the braces. The paddle and gusset plates remained elastic. There was no damage to the welds or connecting angles.

For weld configuration A, results were markedly different between Specimen 1 (0.787 in. weld overlap length) and Specimen 2 (no weld overlap). Specimen 2 experienced extensive yielding at the connection before net section rupture at approximately 1.6 in. of displacement. The rupture was at the bottom connection. Welds at the bottom connection were shorter than specified and shorter than at the top connection. Specimen 1 experienced plastic elongation over the length of the HSS before a mid-length brace fracture at approximately 8.9 in. of displacement. Figure 7 shows this contrast in behavior for specimens from the Afifi et al. (2022) and Moreau et al. (2014) test programs. Note that the specimen shown in Figure 7(b) has a conventional connection.

Differences in behavior extended to the measured strains. In Specimen 1, the strains were initially higher at the top and bottom connections, reached peak strains, and then dropped off. Meanwhile, the strains at mid-length steadily increased for the duration of the test. In Specimen 2, strains were initially higher at the top connection, but the strains increased exponentially and were the highest at the bottom connection at the point of failure (i.e., fracture). Strains at Specimen 2 mid-length were less than half of the strain

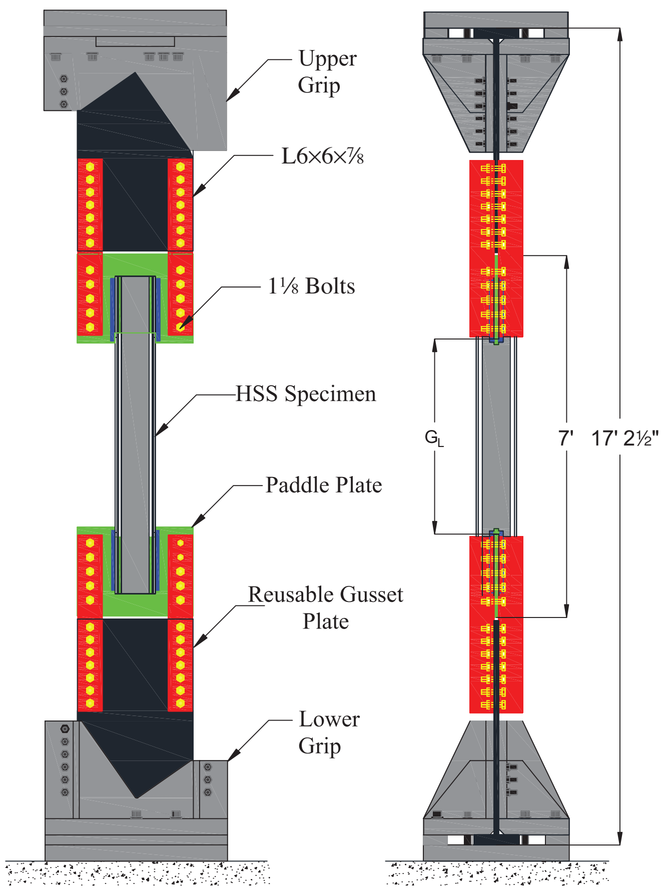

Fig. 6. Schematic of monotonic test setup.

at the top connection. Overall, Specimen 1 experienced a maximum strain of 55,000 με compared to only 35,000 με for Specimen 2.

The contrast in behavior was similar for Specimen 3 (0.787 in. weld overlap length) and Specimen 4 (no weld overlap), both of which used the smaller and longer welds for configuration B. Specimen 4 fractured on net section at approximately 1.6 in. of displacement. Specimen 3 yielded and fractured near mid-length of the brace, near 6.2 in. of displacement. Strain histories were also similar to those seen for weld configuration A. However, strains exceeded 80,000 με for Specimen 4 before fracture.

The test results confirmed expected effects of weld size and length. Specimens had different gage lengths for weld configurations A and B, so normalized load-displacement curves were compared. Specimen 1 failed at 19.2% brace strain compared to 22.3% for Specimen 3 with the smaller, longer welds. Specimen 3 also 1.5% higher tensile strength than Specimen 1; this was attributed to shear lag effects. A similar pattern was observed for Specimens 2 and 4, again with an increase in brace strains (2%) for the longer compared to the shorter weld.

The weld overlap length was the most critical parameter. Specimens with 0.787 in. weld overlap attained full capacity (yield) of the HSS member before fracturing at mid-length, away from the connection. No weld overlap resulted in localized yielding, necking, and fracture at the net section. As noted previously, for the same weld overlap length, the specimens with the longer welds experienced higher tensile loads and larger brace strains.

(a) SHG specimen *(b) Conventional specimen*

Fig. 7. Extensive yielding along length of HSS and eventual fracture in SHG specimen from the Afifi et al. (2022) study, in contrast with fracture of conventional specimen at the connection from a Moreau et al. (2014) test.

The test results were supplemented with additional finite element (FE) investigations. Afifi et al. (2022) first conducted post-testing calibration of the FE models against the test results. Then, 25 FE models provided additional insight into the behavior of different SHG configurations for square HSS braces. The analysis results showed that thinner gusset plates are preferred. With the narrower slots in the HSS, loads are transferred more uniformly from the gusset plate to the HSS. The analyses also confirmed that smaller size, longer welds have lower inelastic demands at the connection and more extensive yielding over the brace length. Additional conclusions and recommendations can be found in Afifi et al. (2022).

Design and Detailing of SHG Connections

The research team sought to improve upon existing design and detailing recommendations for SHG connections. SHG connections prevent HSS net section rupture at the connections during the "high force tension cycles (anticipated strengths) of a seismic event" while eliminating the need to reinforce the net section to satisfy capacity design requirements (Afifi et al., 2023). The design recommendation development required additional parametric studies, as the investigations thus far "did not assess the effects of varying different elements simultaneously" (Afifi et al., 2023). In this parametric study, critical locations along the brace and connection were assessed, further evaluating important parameters for load transfer from the HSS to the plate.

The extensive parametric study was designed based on limits and most influential parameters from the research team's prior work. The studies to date had a limited number of square sizes, so the team explored 15 different HSS sizes. The HSS ranged from 16 in. square and 0.866 in. thick to 3 in. square and 0.189 in. thick (HSS 406×406×22 to HSS 76×76×4.8). Each HSS was analyzed with 2 weld configurations, 10 weld overlap lengths, 5 plate thicknesses, and 5 weld sizes. The gap length was kept at the 1.18 in. recommended by Martinez-Saucedo (2007). Afifi et al. (2023) noted that the gap met "fabrication tolerances found in common practice" and that keeping the value constant would minimize computations. The material properties (e.g., ASTM A1085 for the HSS) were also kept constant and consistent with Afifi et al. (2022). Capacity design requirements dictated the ranges for certain parameters. Weld size and length were chosen to be adequate for base-metal limit states and weld-metal fracture. Gusset plate thicknesses were also chosen such that yielding would not occur in the plate. Afifi et al. (2023) also noted that the "range for each parameter was chosen to provide a representative sample size while optimizing the needed computational time and cost." Further details of the parametric study can be found in Afifi et al. (2023).

The finite element modeling was as described in Afifi et al. (2021, 2022). Some highlights of the modeling included the stress-strain properties and gage length. True stress-strain curves were based on coupon data from the studies reported in Afifi et al. (2022). Stress-strain properties, accounting for the corners of the HSS and the longitudinal residual stress distribution, were based on Koval (2018). For comparison purposes, brace gage lengths were kept constant—that is, the distance between the HSS slot and brace mid-length was constant across the FE models.

The FE models were validated against prior work. FE model predictions were compared to experiments by Moreau et al. (2014) and Afifi et al. (2022) and prior numerical studies (e.g., Afifi et al., 2021, 2022). The FE model "accurately predicted" the overall connection response as well as location of fracture (e.g., at connection or brace mid-length) for braces with SHG connections with different overlap lengths.

Primary observations from the study related to load transfer and load overlap length. Free body cuts were used to examine load or force transfer through the brace and connection. Each critical location was assigned a "load participation factor," a percentage of load attributed to that connection element. One observation was that the weld load participation factor "increased uniformly with an extension of the weld overlap length" within a range of parameters (Afifi et al., 2023). Meanwhile, increases in weld overlap length showed some improvement in ductility, delaying displacement at failure when the fracture was at the connection. However, beyond the weld overlap length attributed to brace yielding and fracture in gross cross section, there was no benefit or increase in ductility with increase in weld overlap length. For additional results, refer to Afifi et al. (2023).

The main findings formed the basis for the proposed design methodology for the SHG brace connections. The expected, or probable, brace resistance is determined. The minimum weld length for the connection is chosen so as to avoid block shear rupture of the HSS at the connection. Then other components such as gusset plate thickness and weld size are selected based on the chosen weld length. The weld overlap length is chosen so that fracture will occur in at brace mid-length instead of at the connection. The research team's equation for minimum weld overlap length is based on the ratio of HSS effective net area to gross area and the slot thickness. Meanwhile, detailing requirements include a standard 1.18 in. gap as recommended by Martinez-Saucedo (2007), correlating to typical fabrication tolerances. The gusset plate slot width is the HSS outer dimension plus 0.118 in., also based on typical fabrication tolerances. Details of these and other requirements can be found in Afifi et al. (2023).

Validation included design and detailing of three braces and their SHG connections following the proposed design and detailing methods. Full FE models were created of the braces and their SHG connections. The models were subjected to a cyclic load history of increasing displacements, using a protocol similar to that for the long brace presented in Moreau et al. (2014) and Afifi et al. (2021). The three FE models exhibited the desired behavior, with buckling and fracturing at the mid-length plastic hinge. For details of the model and validation, refer to Afifi et al. (2023).

Discussion

Several numerical and experimental studies demonstrated the viability of the SHG connection, provided insight into important parameters, and supported the development of design and detailing guidelines. HSS width and thickness, plate thickness, weld size and length, weld overlap length, and gap length are primary factors in the performance of SHG connections. The proposed design method includes determination of the target weld overlap length, at which fracture occurs at brace mid-length rather than the net section at the connection. Numerical simulations of braces designed and detailed using the proposed method are able to sustain cyclic load reversals until buckling and fracturing at a mid-length plastic hinge.

FUTURE RESEARCH

The research team has advanced design of braced frame structures through research and design development for braces with intentional eccentricity (BIEs) and slotted-hidden-gap (SHG) connections. Full-scale experimental evaluation, supplementary finite element studies, and nonlinear dynamic system analyses have demonstrated the benefits of BIEs and highlighted areas requiring additional investigation. Design procedures, details, and performance of eccentering assemblies and connections are among the areas for future study. Afifi et al. (2022) investigated constructability of the SHG braces and connections, but this topic needs additional study as well. Another potential research topic is the influence of compression loading and gusset detailing of SHG connections for HSS braces.

ACKNOWLEDGMENTS

Thank you to Dr. Colin Rogers and Dr. Robert Tremblay for their contributions to this article. The work of Ph.D. graduates Mohamed Afifi and Andrés González Ureña, as well as Master's graduate Rolando Moreau, is also recognized, along with the technicians and engineers at the Hydro-Quebec Structural Engineering Laboratory at Polytechnique Montreal, as well as undergraduate and graduate research assistants from Polytechnique Montreal and McGill University. The research is sponsored by the Natural Sciences and Engineering Research Council of Canada (NSERC) and the Fonds de recherche du Québec-Nature et technologies (FRQ-NT). The researchers would also like to thank DPHV Structural Consultants, Constructions Proco, ADF Group Inc., and Atlas Tube for their technical and financial support. Any findings or recommendations are those of the researchers and do not necessarily reflect the views of the sponsors.

REFERENCES

Afifi, M., Moreau, R., Tremblay, R., and Rogers, C.A. (2021), "Evaluation of the Slotted-Hidden-Gap (SHG) Connection for Square HSS Brace Members," *Journal of Constructional Steel Research*, Vol. 179, No. 21, 106548. https://doi.org/10 .1016/j.jcsr.2021.106548

Afifi, M., Tremblay, R., and Rogers, C.A. (2022), "Numerical and Experimental Investigation of Slotted-Hidden-Gap (SHG) Connection for Square HSS Brace Members," *Journal of Constructional Steel Research*, Vol. 192, No. 4, 107234. https://doi.org/10.1016/j.jcsr.2022.107234

Afifi, M., Tremblay, R., and Rogers, C.A. (2023), "Design and Detailing Recommendations of Slotted-Hidden-Gap (SHG) Connection for Square HSS Brace Members," *Journal of Structural Engineering*, ASCE, Vol. 149, No. 2, 04022249.

ASTM (2015), *Standard Specification for Cold-Formed Welded Carbon Steel Hollow Structural Sections (HSS),* ASTM A1085/1085M, ASTM International, West Conshohocken, Pa.

ASTM (2021), *Standard Specification for High-Strength Low-Alloy Columbium-Vanadium Structural Steel*, ASTM A572/A572M-21, ASTM International, West Conshohocken, Pa.

CSA (2018), *General Requirements for Rolled or Welded Structural Quality Steel/Structural Quality Steel*, G40.20-13/G40.21-13 (R2018), Canadian Standards Association, Toronto, Canada.

CSA (2019), *Design of Steel Structures*, S16-14 (R2019), Canadian Standards Association, Toronto, Canada.

González Ureña, A., Tremblay, R., and Rogers, C.A. (2021), "Earthquake-Resistant Design of Steel Frames with Intentionally Eccentric Braces," *Journal of Constructional Steel Research*, Vol. 178, 106483. https://doi.org/10.1016/j.jcsr.2020.106483

González Ureña, A., Tremblay, R., and Rogers, C.A. (2022), "Experimental and Numerical Study of Square HSS BIEs under Cyclic Loading," *Engineering Structures*, Vol. 252, 113669. https://doi.org/10.1016/j.engstruct.2021.113669

Koval, I. (2018), "Accounting for Cold Working and Residual Stress Effects on the Axial Strength of HSS Bracing Members," M.Sc. Thesis, Département des génies civil, géologique et des mines, École Polytechnique de Montréal, Montréal, Canada.

Martinez-Saucedo, G. (2007), "Slotted End Connections to Hollow Sections," Ph.D. dissertation, Department of Civil Engineering, University of Toronto, Toronto, Canada.

Martinez-Saucedo, G., Packer, J.A., and Christopoulos, C. (2008), "Gusset Plate Connections to Circular Hollow Section Braces under Inelastic Cyclic Loading," *Journal of Structural Engineering*, ASCE, Vol. 134, No. 7, pp. 1252–1258.

Mitsui, Y., Kurobane, Y., and Endoh, K. (1985), "Experimental Study on Ultimate Strength and Deformation Capacity of Welded Tube-to-Through Gusset Plate Joints," *Journal of Structural Engineering*, ASCE, Vol. 31, No. B, pp. 145–156.

Moreau, R., Tremblay, R., and Rogers, C.A. (2014), "Evaluation of the 'Modified-Hidden-Gap' Connection for Square HSS Brace Members," Research Report, Department of Civil Engineering, McGill University, Quebec, Canada.

Okazaki, T., Lignos, D.G., Hikino, T., and Kajiwara, K. (2013), "Dynamic Response of a Chevron Concentrically Braced Frame," *Journal of Structural Engineering*, ASCE, Vol. 139, No. 4, pp. 515–525.

Packer, J.A., Chiew, S.P., Tremblay, R., and Martinez-Saucedo, G. (2010), "Effect of Material Properties on Hollow Section Performance," *Proceedings of the Institution of Civil Engineering: Structures and Buildings*, Vol. 163, No. 6, pp. 375–390.

Skalomenos, K.A., Inamasu, H., Shimada, H., and Nakashima M. (2017), "Development of a Steel Brace with Intentional Eccentricity and Experimental Validation," *Journal of Structural Engineering*, ASCE, Vol. 143, No. 8, 04017072. https://doi.org/10.1061/(ASCE)ST.1943-541X.0001809